out if higher order basic shapes are used. Surface waviness, apart from the leading edge droop, is small, and the number of surface waves increase with increasing number of basic shapes used in a design. All the designed shapes have a leading edge droop and a washout in incidence in the outboard portion with the tip vicinity showing negative incidences. This should, as in the basic shapes, be helpful in delaying tip stall problems.

Numerical calculations also show that combinations of higher order basic shapes or combinations of larger number of basic shapes gradually push the pressure peak outboard, increase the peak intensity, and by acting on the forward facing drooped portion of the leading edge produce a thrust force that alleviates drag, Fig. 4. Table 1 shows that the leading edge thrust lost by prescribing an attachment line at the leading edge is admirably made up by the pressures acting on the droop, and drag values quite close to the plane delta with full suction are attainable. Also, from Table 1, for even combinations, the wing incidence increases as higher order basic shapes are used. For odd combinations, the opposite trend is true.

Many of the designed shapes in Fig. 3 appear to be of practical use because of small surface waviness and favourable twist near the leading edge. In practice, the plane delta will never develop full leading edge thrust, which may be almost half the magnitude of the total drag for low aspect ratios,[5] due to flow separation. Hence, the conically cambered delta with its drooped leading edges will provide definite improvements in the lift to drag ratio in a real flow. The designs of this Note do not exhibit pronounced waviness as in Refs. 2 and 4, where the shapes were obtained by superimposing known pressure distributions, and hence our wing shapes are less conducive to produce shocks due to compressions on the wing surface.

References

[1]Bera, R. K., "The Slender Delta Wing with Conical Camber," *Journal of Aircraft*, Vol. 12, No. 4, April 1974, pp. 245–247.

[2]Smith, J. H. B. and Mangler, K. W., "The Use of Conical Camber to Produce Flow Attachment at the Leading Edge of a Delta Wing and to Minimize Lift Dependent Drag at Sonic and Supersonic Speeds," R and M 3289, 1963, Aeronautical Research Council, London.

[3]Weber, J., "Design of Warped Slender Wings with Attachment Lines Along the Leading Edge," R and M 3406, 1965, Aeronautical Research Council, London.

[4]Tsien, S. H., "The Supersonic Conical Wing of Minimum Drag," *Journal of the Aeronautical Sciences*, Vol. 22, No. 12, Dec. 1955, pp. 805–817.

[5]Jones, R. T., "Properties of Low Aspect Ratio Pointed Wings at Speeds Above and Below the Speed of Sound," Rept. 835, 1946, NACA.

Stress Diffusion in Thick Stiffened Panels

Grant P. Steven*

University of Sydney, Sydney, Australia.

Introduction

STIFFENED panels are becoming a more common structural component not only in aircraft but in civil and other transport type structures. In all applications of such structures the skin thickness between stiffeners is becoming greater and this trend makes the use of the traditional lumped stiffener[1-7] more inappropriate as will be shown herein. Finite element methods can obviously be used. However, there is always room for a closed-form solution which can illustrate more rapidly the effect of increased skin thickness in relation to the stiffener cross-sectional area.

Received December 19, 1973; revision received August 20, 1974.

Index categories: Aircraft Structural Design (Including Loads); Structural Static Analysis.

*Lecturer, Department of Aeronautical Engineering.

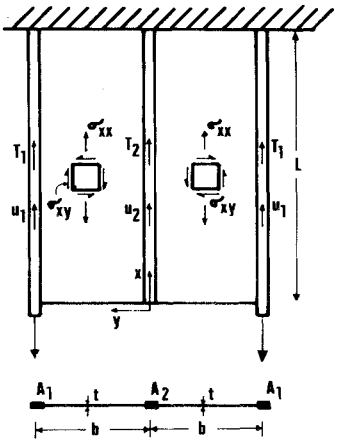

Fig. 1 Three-stringer panel showing loading and internal stress and displacement values.

In this work the skin is allowed to sustain a more natural fraction of the direct stress capacity of the panel, and its area is not lumped with the stiffeners. It can be shown that the rates at which concentrated loads diffuse into the panel are considerably altered by this technique and compare much more favorably with finite element and experimental results.

The three-stringer panel is chosen as being the simplest with which the improved stress diffusion theory can be presented. Five and seven-stringer panels have also been studied and the comments which are applied to this three-stringer panel can be applied to the others also. A sketch of the panel showing the internal stress system is given in Fig. 1. The following assumptions are made in order that the analysis can proceed. 1) The stiffeners carry only direct stress denoted by their tensions T_1 and T_2 which are functions of x. 2) The skin carries direct stress and shear stress, where the magnitude of the direct stress is constant with y and at the same level as the stress in the center unloaded stringer. This gives the correct boundary condition that direct stress be zero at the loaded end $x = 0$. 3) The panel has an infinite transverse stiffness.

On the basis of Assumption 2 and using the x-direction equilibrium equation of plane stress;

$$\partial\sigma_{xx}/\partial x + \partial\sigma_{xy}/\partial y = 0 \tag{1}$$

it can be said that since σ_{xx} is not a function of y then $\partial\sigma_{xx}/\partial x$ is not a function of y and therefore $\sigma_{xy} = -\int \partial\sigma_{xx}/\partial x \, dy$ illustrates that σ_{xy} will be a linear function of y which can be denoted as,

$$\sigma_{xy} = \tau_0 + y/b\,\tau_1 \tag{2}$$

where τ_0 and τ_1 are functions of x only. The shear strain, using Assumption 3 is;

$$\epsilon_{xy} = \frac{\partial u}{\partial y} = \frac{\sigma_{xy}}{G} \tag{3}$$

and integrating between the limits $y = 0$ and b yields

$$G(u_1 - u_2) = \tau_0 b + \tau_1 b/2 \tag{4}$$

Stress displacement relationships for the direct stresses are, using Assumption 2 for the skin;

$$T_1/A_1 = E\,du_1/dx,\ T_2/A_2 = E\,du_2/dx,$$
$$\sigma_{xx} = \sigma = E\,du_2/dx = T_2/A_2 \tag{5}$$

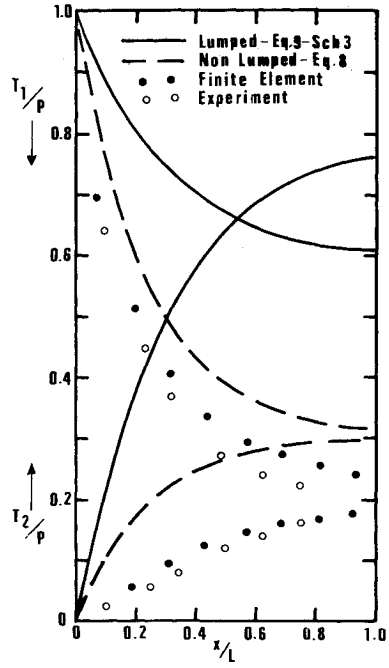

Fig. 2 Variation of stringer tensions with length for loading system in Fig. 1.

Equilibrium, both over-all and inter-element, yields the following equations

$$\begin{aligned} 2P &= 2T_1 + T_2 + 2bt\sigma \\ dT_1/dx + bt(d\sigma/dx) &= \tau_0 t \\ dT_1/dx &= \tau_0 t + \tau_1 t \end{aligned} \tag{6}$$

The sets of Eqs. (4–6) describe fully the state of stress and displacement within the structure subject to the initial assumptions. Reducing these to an ordinary second-order differential equation in T_1 it is found that,

$$\begin{aligned} d^2T_1/dx^2 - \alpha^2 T_1 &= -[P2Gl/bE(A_2 + bt)] \\ \alpha^2 &= \frac{Gl}{EA_1 b}\left(\frac{2A_1 + A_2 + 2bt}{A_2 + bt}\right) \end{aligned} \tag{7}$$

In order to compare the solution of Eq. (7) with experimental results a finite length panel of length L is used giving the boundary conditions; $T_1 = P$ at $x = 0$ and $u_1 = u_2 = 0$; i.e., $\tau_1 = \tau_0 = 0$ at $x = L$. Subject to these boundary conditions the solution of Eq. (7) becomes,

$$T_1 = P\left[K\left(\frac{e^{-2\alpha L}e^{\alpha x} + e^{-\alpha x}}{1 + e^{-2\alpha L}}\right) + (1 - K)\right] \tag{8a}$$

$$T_2 = \frac{2P - 2T_1}{[1 + 2bt/A_2]} \tag{8b}$$

$$\sigma_{xy} = 2PK\alpha\left[\frac{1/2l + y/A_2}{1 + 2bt/A_2}\right]\left[\frac{e^{-2\alpha L}e^{\alpha x} - e^{-\alpha x}}{1 + e^{-2\alpha L}}\right] \tag{8c}$$

$$K = 1 - \left[\frac{2}{2 + A_2/A_1 + 2bt/A_1}\right] \tag{8d}$$

If the traditional lumping technique had been used, the stringer areas are modified to A_{1e} and A_{2e} and σ is taken as zero in the skin, thus the shear stress is constant with y in the panel. The solution for this case can be extracted from Eq. (8) by setting $A_1 = A_{1e}$, $A_2 = A_{2e}$ and $bt = 0$ to give,

$$T_1 = P\left[K'\left(\frac{e^{-2\beta L}e^{\beta x} + e^{-\beta x}}{1 + e^{-2\beta L}}\right) + (1 - K')\right] \tag{9a}$$

$$T_2 = 2P - 2T \tag{9b}$$

$$\sigma_{xy} = PK'\alpha/l\left[\frac{e^{-2\beta L}e^{\beta x} - e^{-\beta x}}{1 + e^{-2\beta L}}\right] \tag{9c}$$

$$K' = 1 - \frac{2}{[2 + A_{2e}/A_{1e}]} \tag{9d}$$

$$\beta^2 = Gl/Eb\,[1/A_{1e} + 2/A_{2e}] \tag{9e}$$

The ratio α/β gives an indication of the difference in the rate at which the concentrated loads diffuse into the panel for the two cases, nonlumped and lumped. For the lumping technique there have been various rules which govern how the skin area is to be distributed into the stiffeners. At this point, it would be illustrative to compare the ratio α/β for four possible lumping schemes. It will be assumed that $A_1 = A_2 = A$.

Scheme 1: All skin lumped into center stringer.

$$\begin{aligned} A_{1e} &= A,\ A_{2e} = A + 2bt \\ \alpha/\beta &= \left[\frac{1 + 2bt/A}{1 + bt/A}\right]^{1/2} \end{aligned} \tag{10}$$

Scheme 2: Half skin in any panel lumped into adjacent stringer.

$$\begin{aligned} A_{1e} &= A + bt/2,\ A_{2e} = A + bt \\ \alpha/\beta &= [1 + bt/2A]^{1/2} \end{aligned} \tag{11}$$

Scheme 3: Skin divided evenly between stringers.

$$\begin{aligned} A_{1e} &= A + (2/3)bt,\ A_{2e} = A + (2/3)bt \\ \alpha/\beta &= \left[\frac{(1+(2/3)bt/A)^2}{1 + bt/A}\right]^{1/2} \end{aligned} \tag{12}$$

Scheme 4: All skin lumped into outer stringers.

$$\begin{aligned} A_{1e} &= A + bt,\ A_{2e} = A \\ \alpha/\beta &= 1 \end{aligned}$$

From these values of α/β, it initially would appear that Scheme 4 would give the same diffusion rate; however, if values for the dimensions and properties are substituted into Eqs. (8), (9), it is found that the stringer forces given by Scheme 4, although they diffuse at the improved rate, do not settle down to give a uniform distribution of stress across the panel as one would expect from St. Venant's principle. Schemes 2 and 3 give the best distributions of stress, and it can be seen that these give, for a value of $bt/A = 1$ say, ratios of α/β of 1.21 and 1.18, respectively. These values show that the stringer tensions decay much more rapidly to their mean value if the assumptions of this paper are made, namely, that the skin is allowed to carry some of its direct stress capacity.

In order to investigate this problem further, an experimental three-stringer panel was constructed with a value $bt/A = 1.82$. This was strain gauged and tested for the distribution of stringer tension. Also a finite element model was constructed using 96 three-node elements in plane stress and 24 two-node flange elements to represent the stringers.

In Fig. 2 we see a plot of the stringer tensions with length for this panel. From this we note one of the intrinsic difficulties of comparing the values given by the closed-form solution of this paper and the lumped stringer approach; since the stringers in the lumped technique carry the part of the load that ought to be carried by the skin, stringer tensions are that much larger. However, to eliminate difficulty with stringer tension and plot on the basis of stress, which would thereby give a better terminal correspondence of values, gives rise to too low a stress at the loaded end. Stress is too small since A_{1e} in Stringer 1 is not the true cross sectional area. If A_1 is used instead of A_{1e}, then the values are too high at the built-in end of the panel. Figure 2 illustrates that the closed-form solution presented herein is in good agreement with both experimental and finite element values.

Conclusion

This form of solution has also been evaluated for five and seven stringer panels and, here again, the comparison with finite element solutions is good. Thus, by allowing the skin in a stiffened panel to carry some of its direct stress capacity, a more accurate distribution of the internal stress system can be obtained. For the panel tested, the shear stress distribution gives a value of stress in the skin, adjacent to the load application point, which is 120% greater than that predicted by the simple lumping Scheme 3. Since the analysis technique used herein gives a better approximation to the internal stress system in the panel, failure of the panel by shear buckling can now be more accurately predicted.

References

[1]Kuhn, P., *Stresses in Aircraft and Shell Structures*, McGraw-Hill, N.Y. 1956.

[2]Cox, H. L., Smith, H. E., and Conway, C. G., "Diffusion of Concentrated Loads into Monocoque Structures," R & M 1780, 1937, Royal Aircraft Establishment, Farnborough, England.

[3]Cox, H. L., "Diffusion of Concentrated Loads into Monocoque Structures," R & M 1860, 1938, Royal Aircraft Establishment, Farnborough, England.

[4]Duncan, W. J., "Diffusion of Load in Certain Sheet-Stringer Combinations," R & M 1825, 1938, Royal Aircraft Establishment, Farnborough, England.

[5]Hadji-Argyris, J., "Diffusion of Symmetrical Loads into Stiffened Parallel Panels with Constant Area Edge Members," R & M 2038, 1944, Royal Aircraft Establishment, Farnborough, England.

[6]Hadji-Argyris, J. and Cox, H. L., "Diffusion of Load into Flat Stiffened Panels of Varying Cross-Section," R & M 1969, 1944, Royal Aircraft Establishment, Farnborough, England.

[7]Argyris, J. H., "Diffusion of Antisymmetrical Loads into, and Bending under, Transverse Loads of Parallel Stiffened Panels," R & M 2822, 1946, Royal Aircraft Establishment, Farnborough, England.

DECEMBER 1974 J. AIRCRAFT VOL. 11, NO. 12

Technical Comments

Comment on "Wind Effects on Electrostatic Autopilots"

Maynard L. Hill* and William A. Hoppel†
The Johns Hopkins University Applied Physics Laboratory, Silver Spring, Md.

SULLIVAN[1] recently described some wind-tunnel experiments designed to simulate the current generated by ionizers used in Electric Field Stabilizers. As originally demonstrated by Hill,[2] the vertical fair-weather atmospheric electric field can be used as a reference for aircraft stabilization. The experiments described by Sullivan measure the output currents generated by two radioactive sources placed at the ends of a mounting board and placed in a wind tunnel so that the ends of the board could be rotated in a plane perpendicular to the air flow. An electric field across the tunnel simulated the earth's vertical electric field. The output current was then measured as a function of wind velocity and angle of orientation of the mounting board with respect to the direction of the electric field. The entire system simulates an aircraft with ionizers on the wing tip at various speeds and angles of bank. The experiment is a valid one and does demonstrate the dependence of the output current on velocity and angle of bank. However, we believe that the analysis given in the paper to describe the velocity dependence is based on an erroneous physical picture of the current generating mechanism. The basic difference between our understanding of the radioactive probe and the analysis given by Sullivan is as follows.

1) Sullivan's analysis implies that a major source of current originates downstream from the ionizer and that the ions flow back to the body along the field lines. Mathematically this is evidenced in both the expression for the "ionized pair density," ρ, which is calculated for the region downstream where the ionization rate q is zero and also in the limits of integration of Eq. (10) in Sullivan's paper. We maintain that the current originates primarily by the action of the electric field on the highly ionized region just above the ionizing probe. Ionic velocities resulting from the mobility of an ion in the atmospheric electric field are less than a few meters per second thus preventing the return of ions to the aircraft for speeds above a few meters per second. Furthermore, the radioactive sources on aircraft are insulated so that only current which originates at the ionizer flows through the amplifier.

2) The velocity dependence in Sullivan's analysis, Eq. (11), arises from the decay of ion densities downstream by recombination. We propose that the ion density downstream of the probe is irrelevant and that the velocity dependence arises from the removal of the "shielding charge" which develops at the outer boundary of the region of high ionization. If the velocity is very low, one polarity of ion will be drawn out of the highly ionized layer and the other polarity ion will be repelled to the probe. This results in a very low field in the highly ionized region with a highly charged shielding layer existing at the outer

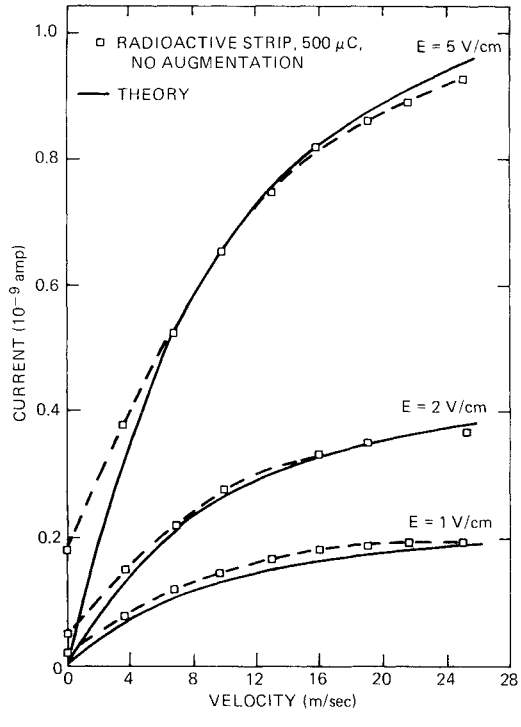

Fig. 1 Current as a function of velocity for electric field values of 1, 2, and 5 v per cm. Solid lines are calculated from Eq. (1).

Received July 8, 1974.
Index category: Aircraft Handling, Stability, and Control.
*Supervisor, RPV Flight Research. Member AIAA.
†Permanent Address—Naval Research Laboratory.